Examination of the validity of the atlas-informed approach to functional parcellation: a resting functional MRI study

Tien-Wen Lee[a,b,c] and Shao-Wei Xue[a,b]

With the advancement in MRI, functional parcellation (FP) of brain structure(s) has become an important topic. However, the large number of voxels is a major obstacle. A-priori partitioning of the brain into several regions of interest (ROIs) is the main data-reduction strategy to simplify brain informatics. This study aims to examine the validity of ROI-based approach to FP by exploring the concordance of the relative distance structures between voxel-wise (raw data) and atlas-informed analyses. Structural and resting state functional MRI (rfMRI) scans of 26 right-handed healthy individuals were selected from the Rockland dataset. Four target regions were included in the analyses, that is, left and right thalamus and amygdala. For each voxel in the target region, four classes of correlation maps (sampling strategies) were constructed from the rfMRI: whole brain, cortex, 150 ROIs, and 70 ROIs (ROIs are informed by anatomical atlases). The relative distance metric between two different voxels was defined as the mean absolute difference of their associated correlation maps. Considering all the possible pairs of voxels in a target region, the relative distance structure was derived and stored in a matrix (distance map). For every target region, the distance maps were very similar across the four classes of sampling strategies, with the grand mean correlation coefficient reaching 0.95. The results confirm the validity of previous ROI-based analyses of rfMRI data in FP. The rationale and limitation are discussed and an analytic strategy of whole-brain FP is proposed. *NeuroReport* **28:649–653** **Copyright © 2017 Wolters Kluwer Health, Inc. All rights reserved.**

NeuroReport 2017, **28**:649–653

Keywords: amygdala, functional connectivity, functional MRI, functional parcellation, resting functional MRI, thalamus

[a]Department of Psychology, Center for Cognition and Brain Disorders, Hangzhou Normal University, [b]Zhejiang Key Laboratory for Research in Assessment of Cognitive Impairments, Hangzhou, Zhejiang Province, China and [c]Department of Psychiatry, Dajia Lee's General Hospital, Lee's Medical Corporation, Taichung, Taiwan

Correspondence to Tien-Wen Lee, MD, PhD, Room 301, Shuyuan Building No. 19, Yuhangtang Road No. 2318, Hangzhou 311121, Zhejiang Province, China
Tel: +86 152 571 52036; fax: +86 571 288 67717;
e-mail: dwlee_ibru@yahoo.com.tw

Received 20 April 2017 **accepted** 26 April 2017

Introduction

Brain tissues that carry out similar neural operations are believed to aggregate together. The delineation of homogenous cortical and subcortical (sub) regions has been attempted from various perspectives, such as histology, white matter bundles, and anatomical landmarks. With the advancement of neuroimaging tools, the segmentation of brain structure(s) on the basis of functional characteristics has become a topic of both theoretical and clinical importance. Functional parcellation (FP) is generally achieved by examining the transitions in the patterns of predefined interareal relationships. Consider the FP of the thalamus through a voxel-wise functional correlation (FC) map as an example: the neural activity of each voxel is correlated with those of the remaining voxels to constitute a whole-brain correlation map. The adjacent voxels with similar FC patterns (and hence smaller 'relative distance', described later and in the Participants and methods section) can be grouped together as a cluster, whereas the voxels indicating the transition of different FC patterns may illustrate the boundary and distinct functional clusters are expected to have larger relative distances. Several delicate algorithms have been developed [1–4], but a consensus has not been reached on the optimal FP strategy. A major challenge for FP (especially FP of the whole brain) lies in the large voxel number of functional imaging data. In terms of functional MRI (fMRI), whole-brain scanning may involve tens to hundreds of thousands of voxels. It is consequently a common practice to adopt a data-reduction strategy. Among these strategies, the established anatomical atlases that already partition the brain on the basis of landmarks and/or histology are widely applied, but their validity is still in debate [5–10]. Using anatomical atlases, the resolution can be reduced from the voxel to the region of interest (ROI), usually in the range of tens to hundreds.

It is acknowledged that functionally specialized brain regions have limited correspondence with brain areas delineated by anatomical landmarks and cytoarchitectonic structures [5]. Despite the flawed biological plausibility of the ROI-based approach, the possibility that a target brain region can still be reasonably partitioned on the basis of the abridged information cannot be excluded. The optimism arises from the concordant results of seed-based and ROI-based analyses in other research areas (e.g. modularity analysis) [8,11–15]. Consider parcellating the thalamus into subregions as an example. For a particular voxel in the thalamus, the FC maps derived from the whole-brain voxels and the atlas of 90 ROIs are obviously quite different. Nevertheless, it is the relative

0959-4965 Copyright © 2017 Wolters Kluwer Health, Inc. All rights reserved.
DOI: 10.1097/WNR.0000000000000808

Copyright © 2017 Wolters Kluwer Health, Inc. All rights reserved.

distance structure (which will be introduced below and in the Participants and methods section) among the voxels in the thalamus that accounts for FP. If the above two approaches yield the same relative distance structure, their thalamus parcellation results would be identical. In other words, even if the ROIs provide only a rough (and often inaccurate) cortical representation of homogeneous functional areas, the information might still be adequate to guide FP. This conjecture demands empirical examination and is the purpose of this research. If the assumption is confirmed, it may clarify the concern about data reduction in previous literature and may also help refine the FP strategy of the whole brain.

It is well established that in the resting state, the brain has stable patterns of spontaneous activity that are organized as modular structures [12,13]. Although situated at lower frequency ranges, the blood-oxygen-level-dependent (BOLD) dynamics are very informative [16]. This research used resting state functional MRI (rfMRI) and FC analysis. Four classes of FC maps were constructed across four different sampling strategies, namely, whole brain (hundreds of thousands of voxels), cortex (tens of thousands of voxels), 150 ROIs (Destrieux Atlas), and 70 ROIs (Desikan-Killiany Atlas). The 'distance' between two voxels in a target region is defined as the mean difference of the two associated FC maps. The relative distance structure (distance map) of a particular target region can be elucidated by incorporating the distance metrics of all the possible voxel pairs into a summarized matrix. Four target regions (left and right thalamus; left and right and amygdala) were selected to examine the hypothesis that the relative distance structures among the voxels of a brain region are retained over the four different sampling strategies (i.e. four classes of correlation maps with three different spatial resolutions: voxel, 150 ROIs, and 70 ROIs). For each target region, the 'distance map' obtained from the voxel-based analysis serves as a reference/standard that is compared with the counterparts derived from the ROI-based analyses. Our hypothesis is that if the distance maps of the voxel-wise and ROI-based approaches are similar, the validity of atlas-informed, ROI-based FP is supported.

Participants and methods

Participants

A total of 26 right-handed healthy individuals were selected from the dataset of the Rockland sample (Enhanced Nathan Kline Institute-Rockland Sample); their mean age was 26.3 years. The data source used by this study fulfilled the criteria of 'Nathan Kline Institute-Rockland Sample Neuroimaging Data Release'. The institutional ethics committee approved this project.

MRI data acquisition and preprocessing

T1-weighted structural MRI (sMRI) and rfMRI were included in the analysis. All MRI images covered the whole brain and were acquired by the 3.0 T Siemens Magnetom Trio Tim system (Siemens, Erlangen, Germany). The detailed scanning protocol can be found at: *http://fcon_1000.projects.nitrc.org/indi/pro/nki.html* and the parameters are briefly summarized here. A high-resolution MPRAGE sagittal sMRI was used to facilitate anatomical description and to register rfMRI data (TR, 2500 ms; TE, 3.1 ms; flip angle, 8°; FOV, 256×256 mm; slice-thickness, 1.0 mm; voxel size, $1 \times 1 \times 1$ mm^3; number of slices, 192). Sequential T2*-weighted transversal echo planar images (EPIs) were recorded (TR, 2.5 s; TE, 30 ms; flip angle, 80°; FOV, 216×216 mm; slice-thickness, 3.0 mm; voxel size, $3 \times 3 \times 3$ mm^3; number of slices, 38) to trace dynamic changes of the BOLD in resting state. A total of 260 whole-brain EPI images were collected for $\sim$10 min and the first five EPI volumes were discarded to allow for signal equilibrium.

FreeSurfer was applied to T1-weighted sMRI to segment gray matter and white matter and to parcellate the cortical mantle into 70 (Desikan-Killiany Atlas) and 150 (Destrieux Atlas) ROIs [17,18]. Four subcortical structures were extracted as target regions, including the left and right thalamus and the left and right amygdala. The average BOLD time course in each ROI was prepared to represent the simplified version of cortical activities. The Analysis of Functional NeuroImages software package was used to process the rfMRI data [19] and the analytic streamline developed by Jo *et al.* [20] was adopted to prepare the rfMRI images [7,8]. The preprocessing steps of rfMRI comprised despike, slice-time correction, realignment (motion corrected), registration to T1 anatomy, spatial smoothing (6 mm), and bandpass filtering to 0.01–0.1 Hz. Several regressors were created and modeled as nuisance variables, comprising six movement parameters, third-order polynomials to fit baseline drift, and tissue-based regressors of white matter (global and local) and ventricles [20]. The tissue-based regressors were constructed using the segmentation results obtained from FreeSurfer.

Functional correlation map construction and similarity analysis

Let us start from the left thalamus, and the same analytic stream was applied to the other three target regions. Four classes of FC maps were constructed by Pearson's correlation: the BOLD time course of each voxel in the left thalamus was correlated with (i) the BOLD time course of the voxels in the whole brain, (ii) the BOLD time course of the voxels in the cortex, and (iii) the averaged BOLD signals in the ROIs derived from the two atlases mentioned above. For each class, 'difference maps' were calculated for each pair of voxels. If the voxel number in the left thalamus was N, then the number of difference maps would be $N \times (N-1)/2$ (divided by 2 because we took the absolute value and the difference map of voxel pair $a-b$ would be the same as that of voxel pair $b-a$).

Copyright © 2017 Wolters Kluwer Health, Inc. All rights reserved.

The 'distance' between two correlation maps, and hence the distance between two voxels in the left thalamus, was defined as the average absolute value of the corresponding difference map. It is noteworthy that the distance in this article is not relevant to physical coordinates; instead, it indicates the degree of discordance between two correlation maps. Each difference map yielded one distance value and the numbers of distance values were the same for all four classes of correlation maps [i.e. $N\times(N-1)/2$]. The distance metrics can be summarized in an N by N matrix named 'distance map' (note that difference and distance maps are distinct in this article). The similarity between the four classes of distance maps was then compared by another correlation analysis of the constituent distance metrics, and the number of comparisons was 6 [i.e. $4\times(4-1)/2$] for each participant. Strong correlations would indicate that the structure of relative distance for the voxels in the left thalamus was retained across the four conditions (sampling strategies), irrespective of the resolution at the voxel or the ROI level.

Results

It was discovered that the distance structures of the four classes of correlation maps were very similar. The main results are summarized in Tables 1 and 2. Across the four target regions (left and right thalamus; left and right amygdala), the overall average correlation values of the 26 participants was 0.95 (SD = 0.03; *d.f.* = 23). The average correlation coefficients for the left thalamus, right thalamus, left amygdala, and right amygdala were 0.94 (SD = 0.03; *d.f.* = 5), 0.95 (SD = 0.03), 0.96 (SD = 0.02), and 0.96 (SD = 0.02), respectively. The distance structures of a randomly selected participants are shown in Fig. 1.

Discussion

The large number of voxels is a major challenge for the FP of brain structures; therefore, several data-reduction strategies are frequently applied, such as regularly spaced seeds and atlas-defined ROIs [4,7]. It has long been a concern that the FP (and other conditions, such as modularity analysis) based on the atlas-informed FC maps (ROI-based approach) may be inaccurate as the correspondence among different methods used to define a functional region is quite limited [5,6]. If the validity of the upstream stage is questionable, the subsequent results could be biased. From the viewpoint of engineering and statistics, however, the critical point is whether the relative distance structures are retained and whether the signal embedded in the atlas-informed ROI-FC map is enough for successful FP. A-priori division of the cortex into homogeneous subregions is obviously desirable, but may not be absolutely necessary for reliable FP of the cortical or subcortical structures, in this case, the thalamus and amygdala. This study compared the relative distance structures over four different conditions, that is, whole-brain voxels, cortical voxels, and 70 and 150 ROIs. It was found that the structures of the relative distance derived from ROI-based analyses were nearly identical to those from whole brain and cortex analyses across the four selected target regions. Our hypothesis was confirmed and the implications of the results could be generalized to other brain regions and to whole-brain FP as described below.

Table 1 Similarity (mean correlation coefficient across 26 participants) between four different classes of correlation maps at left (lower triangle) and right (upper triangle) thalamus

	Atlas I	Atlas II	Whole brain	Cortex
Atlas I	–	0.98	0.90	0.93
Atlas II	0.98	–	0.93	0.96
Whole brain	0.90	0.92	–	0.97
Cortex	0.93	0.96	0.97	–

There are 70 and 150 regions of interest for atlas I and atlas II, respectively.

Table 2 Similarity (mean correlation coefficient across 26 participants) between four different classes of correlation maps at left (lower triangle) and right (upper triangle) amygdala

	Atlas I	Atlas II	Whole brain	Cortex
Atlas I	–	0.99	0.93	0.94
Atlas II	0.99	–	0.95	0.96
Whole brain	0.94	0.95	–	0.98
Cortex	0.94	0.96	0.98	–

There are 70 and 150 regions of interest for atlas I and atlas II, respectively.

Contradictory viewpoints on data reduction in network analyses are noted. On one hand, previous results of ROI-based and voxel-based modular analyses were quite consistent, supporting the usefulness of the ROI-based approach [7,8,12–15]. On the other hand, recent research has suggested that the use of ROIs derived from structural atlases that are not functionally homogeneous 'is extremely damaging to network estimation' [9,10]. How can the above, opposing perspectives be reconciled? We believe that the issue is context or vantage point dependent, and what counts is whether the informatics is enough to achieve the analytic goal. For example, if we intend to carry out modular analysis or FP, an ROI-based approach may be good enough. However, if we intend to investigate directional network interaction, such as causal inference, ROI analysis informed by an anatomical atlas is very likely to yield a faulty conclusion.

What is the theoretical foundation behind the validity of the ROI-based approach of FP? Although an ROI-based data-reduction strategy may lack biological plausibility, it makes sense in statistics. An ROI-based approach is similar to two-stage sampling in which the whole-brain (or cortex) voxels are divided into clusters (ROIs), and then only one sample is selected from each cluster (in this case, the mean value of a particular ROI instead of a randomly selected voxel in that ROI). The statistical vantage point may also provide insight into the concordance of various seed-based and ROI-based analytic

Copyright © 2017 Wolters Kluwer Health, Inc. All rights reserved.

Fig. 1

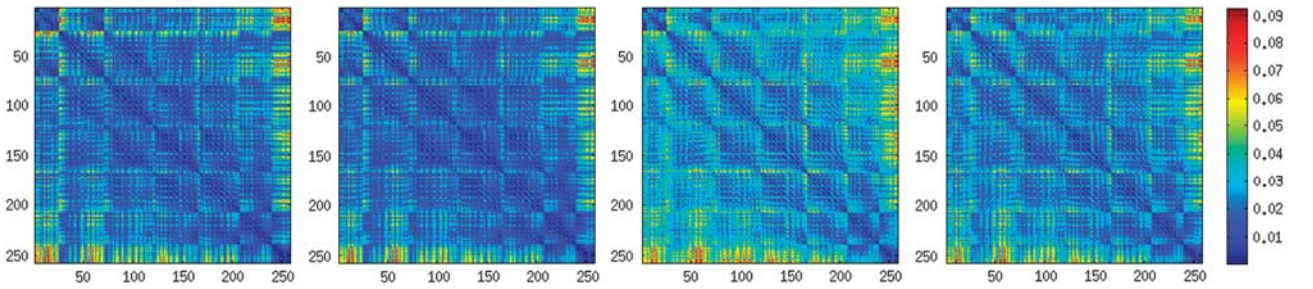

Example illustration of relative distance structures derived from four classes of correlation maps. From left to right: 70 regions of interest (ROIs), 150 ROIs, whole brain and cortex. The data are from a randomly selected participant, and the numbers along the axes are voxel indices of the left thalamus. The color at coordinate (*i*, *j*) indicates the magnitude of the relative distance between voxel *i* and voxel *j*, as shown in the color bar on the right-hand side.

results in previous rfMRI studies. For example, the default-mode network shown by whole-brain correlation with a seed region (in posterior cingulate cortex) was in accordance with that disclosed by modular analysis of the ROI-based correlation matrix [7,8,13]. Mathematicians inferred that unbiased sampling at the level of 1000 is a fair representation of the general population [21], and more samples will not help much to increase the power (the sample number of opinion polls generally obeys the criterion). The metrics at the number of thousands ($70 \times 69/2$; 70 ROIs) was thus good enough to represent the whole brain and the cortex. Knowledge of statistics may provide an alternative reference frame to appraise neuroscientific debates; for example, in some contexts (as shown in the Results section), a rigorous definition of neural nodes for network analysis may not be necessary [6]. The similarity between relative distance structures of the whole brain and cortex resonated with the neuroanatomical fact of intense cortical and subcortical interaction [22].

There are many clustering and community detection algorithms for FP of the brain, and considering each of these algorithms is beyond the scope of this study. We focused on the validity of the data-reduction strategy, which is mediated by an atlas-informed ROI approach and is a prerequisite for credible FP. On the basis of our positive findings, it is possible to perform whole-brain FP in three steps. First, the brain can be divided into several target regions. Second, for each target region, the original resolution (i.e. voxels) is maintained, whereas the rest of the brain can be partitioned into tens of ROIs according to the anatomical atlas. The FP of the target region can be performed on the basis of simplified but still sufficient information. Finally, iteration of the above procedure to the remaining target regions may fulfill automatic FP of the whole brain, with a marked reduction in computation burden and disk space. The application of the above scheme to concatenated individual data may provide group-level representative partitioning. Our findings further suggested that the discrepant results in previous FP and modular research may originate from the algorithms *per se*, whereas the resolution of brain informatics might not play a substantial role. Automatic whole-brain FP may in turn provide a better representation of simplified brain informatics as the partitioning is based on the similarity in BOLD dynamics, which may provide a more solid foundation for further network analyses.

Acknowledgements

Both T.W. Lee and S.W. Xue contributed intellectually to this work and carried out the analysis. T.W. Lee wrote the first draft.

This work was supported by Dajia Lee's General Hospital, Lee's Medical Corporation, Taichung, Taiwan. This study was funded by the Natural Science Foundation of Zhejiang Province Grant LY17H180007; Social Development Project of Hangzhou 20170533B06.

Conflicts of interest

There are no conflicts of interest.

References

1 Shen X, Papademetrisf X, Constable RT. Graph-theory based parcellation of functional subunits in the brain from resting-state fMRI data. *Neuroimage* 2010; **50**:1027–1035.
2 Ryali S, Chen T, Supekar K, Menon V. A parcellation scheme based on von Mises–Fisher distributions and Markov random fields for segmenting brain regions using resting-state fMRI. *Neuroimage* 2013; **65**:83–96.
3 Thirion B, Varoquaux G, Dohmatob E, Poline J-B. Which fMRI clustering gives good brain parcellations? *Front Neurosci* 2014; **8**:167.
4 Wig GS, Laumann TO, Cohen AL, Power JD, Nelson SM, Glasser MF, *et al.* Parcellating an individual subject's cortical and subcortical brain structures using snowball sampling of resting-state correlations. *Cereb Cortex* 2014; **24**:2036–2054.
5 Amunts K, Schleicher A, Burgel U, Mohlberg H, Uylings HB, Zilles K. 'Broca's region revisited: cytoarchitecture and intersubject variability. *J Comp Neurol* 1999; **412**:319–341.
6 Wig GS, Schlaggar BL, Petersen SE. Concepts and principles in the analysis of brain networks. *Ann N Y Acad Sci* 2011; **1224**:126–146.
7 Xue SW, Li D, Weng XC, Northoff G, Li DW. Different neural manifestations of two slow frequency bands in resting functional magnetic resonance imaging: a systemic survey at regional, interregional, and network levels. *Brain Connect* 2014; **4**:242–255.

Copyright © 2017 Wolters Kluwer Health, Inc. All rights reserved.

8 Lee TW, Northoff G, Wu YT. Resting network is composed of more than one neural pattern: an fMRI study. *Neuroscience* 2014; **274**:198–208.
9 Smith SM, Miller KL, Salimi-Khorshidi G, Webster M, Beckmann CF, Nichols TE, *et al*. Network modelling methods for FMRI. *Neuroimage* 2011; **54**:875–891.
10 Stanley ML, Moussa MN, Paolini BM, Lyday RG, Burdette JH, Laurienti PJ. Defining nodes in complex brain networks. *Front Comput Neurosci* 2013; **7**:169.
11 Fransson P. Spontaneous low-frequency BOLD signal fluctuations: an fMRI investigation of the resting-state default mode of brain function hypothesis. *Hum Brain Mapp* 2005; **26**:15–29.
12 Raichle ME, Snyder AZ. A default mode of brain function: a brief history of an evolving idea. *Neuroimage* 2007; **37**:1083–1090. discussion 1097–1089.
13 Moussa MN, Steen MR, Laurienti PJ, Hayasaka S. Consistency of network modules in resting-state FMRI connectome data. *PLoS One* 2012; **7**:e44428.
14 Greicius MD, Supekar K, Menon V, Dougherty RF. Resting-state functional connectivity reflects structural connectivity in the default mode network. *Cereb Cortex* 2009; **19**:72–78.
15 Calhoun VD, Adali T. Multisubject independent component analysis of fMRI: a decade of intrinsic networks, default mode, and neurodiagnostic discovery. *IEEE Rev Biomed Eng* 2012; **5**:60–73.
16 Biswal B, Yetkin FZ, Haughton VM, Hyde JS. Functional connectivity in the motor cortex of resting human brain using echo-planar MRI. *Magn Reson Med* 1995; **34**:537–541.
17 Dale AM, Fischl B, Sereno MI. Cortical surface-based analysis. I. Segmentation and surface reconstruction. *Neuroimage* 1999; **9**:179–194.
18 Fischl B, Sereno MI, Dale AM. Cortical surface-based analysis. II: inflation, flattening, and a surface-based coordinate system. *Neuroimage* 1999; **9**:195–207.
19 Cox RW. AFNI: software for analysis and visualization of functional magnetic resonance neuroimages. *Comput Biomed Res* 1996; **29**:162–173.
20 Jo HJ, Saad ZS, Simmons WK, Milbury LA, Cox RW. Mapping sources of correlation in resting state FMRI, with artifact detection and removal. *Neuroimage* 2010; **52**:571–582.
21 Freedman D, Pisani R, Purves R. *Statistics*. New York, NY: W.W. Norton & Company; 2007.
22 Alexander GE, deLong MR, Strick PL. Parallel organization of functionally segregated circuits linking basal ganglia and cortex. *Annu Rev Neurosci* 1986; **9**:357–381.

Copyright © 2017 Wolters Kluwer Health, Inc. All rights reserved.